CrossMark

Generation of $^4\mathrm{He}_2^*$ Clusters via Neutron-$^3\mathrm{He}$ Absorption Reaction Toward Visualization of Full Velocity Field in Quantum Turbulence

T. Matsushita, et al. *[full author details at the end of the article]*

Abstract

For flow visualization study of quantum turbulence in superfluid $^4\mathrm{He}$, He_2^* excimers are unique tracers which follow only normal-fluid component flow above 1 K. To generate detectable small He_2^* clouds (clusters) required for full-space velocity field measurements, we have adopted a new method based on neutron absorption reaction of $^3\mathrm{He}$ impurities in $^4\mathrm{He}$ and conducted proof-of-principle experiments. Generation of the He_2^* excimers was detected by laser-induced fluorescence using photomultiplier tubes. The fluorescence was observed to increase proportionally to the neutron flux, suggesting that a sufficient amount of He_2^* excimers were generated by neutrons. We also estimated the number of He_2^* excimers possibly generated by γ-rays and found that the relevant contribution was less than 40%. Thus, the majority of the He_2^* excimers was confirmed to be generated via n-$^3\mathrm{He}$ absorption reactions.

Keywords He_2^* clusters · Neutron-$^3\mathrm{He}$ absorption reaction · Quantum turbulence

1 Introduction

Turbulence is a subject which is scientifically and industrially important but whose detail remains unsolved due to its complexity. Therefore, quantum turbulence has attracted many interests not only for the specific novel physics produced by quantized vortices, but as a key to solve the physics of turbulence. Recently, flow visualization using various micron-sized small particles has been developed as a direct and powerful tool to study quantum turbulence in superfluid $^4\mathrm{He}$ [1,2]. Among them, the triplet-state metastable $^4\mathrm{He}$ molecule (excimer) He_2^* has emerged to be a unique tracer which follows only normal-fluid component flow in quantum turbulence. Since an individual excimer is too tiny to be tracked, they must be observed in the form of a cloud.

✉ T. Matsushita
   matsushita@cc.nagoya-u.ac.jp

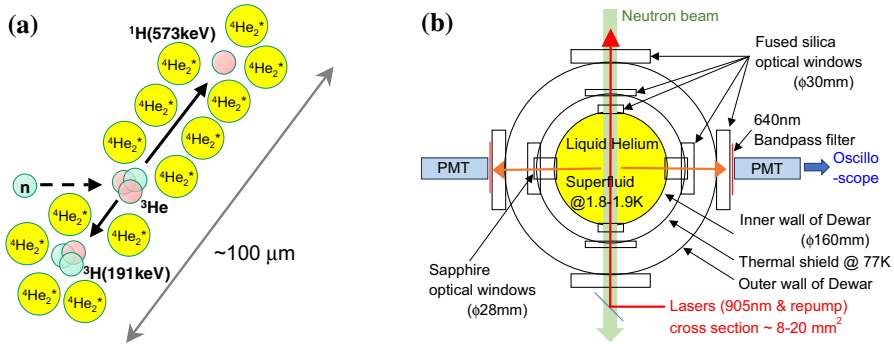Extended author information available on the last page of the article

Fig. 1 **a** Neutron-^{3}He absorption reaction ^{3}He(n,p)^{3}H: n + ^{3}He → ^{1}H + ^{3}H + 764 keV. The number of He$_2^*$ excimers generated along tracks of proton and tritium is expected to be 0.9×10^4 for one reaction. **b** Schematic drawing of the cross section of the cryostat showing the experimental setup. Through a pair of the optical windows, neutron beam and excitation lasers are introduced into superfluid ^{4}He. Resulting fluorescence of triplet He$_2^*$ excimers is observed by photomultiplier tubes with 640 nm bandpass filters from another pair of the optical windows placed in the direction perpendicular to the neutron and laser beams (Color figure online)

In a thermal counterflow experiment using a thin He$_2^*$ excimer line generated by femtosecond laser ionization in liquid He, the transition from laminar to turbulent flows of the normal-fluid component was successfully observed and the profile of the velocity component perpendicular to the line was analyzed [3]. However, full observation of the velocity field requires localized small clouds (clusters) of He$_2^*$ excimers, for which a generation method has not been established so far.

To realize such excimer clusters, the use of the neutron absorption reaction of ^{3}He impurities contained in liquid ^{4}He has been proposed in our project. Expected clusters contain 10^4 excimers in a range of 100 µm. Since excimers do not aggregate and the density in a cluster is much lower than ^{3}He impurities, each He$_2^*$ excimer cluster will be tracked as a single tracer without impeding advantageous properties of He$_2^*$ excimers. They minimally influence the total flow, trace only the normal-fluid component flow above 1 K [3], and gather into quantum vortex lines below 0.5 K [4]. For this proposal, proof-of-principle experiments have been conducted using neutron beams of the research reactor (KUR) at the Institute for Integrated Radiation and Nuclear Science, Kyoto University, and of the Materials and Life Science Experimental Facility (MLF) at the Japan Proton Accelerator Research Complex (J-PARC). In this article, the result confirming excimer generation via n-^{3}He absorption reaction is shown.

2 Experimentals

The proposed method to generate He$_2^*$ excimer clusters is described as follows. Commercially available liquid ^{4}He usually includes ^{3}He atoms in the order of 0.1 ppm as isotopic impurities. By absorption of a neutron, the ^{3}He atom splits into ^{1}H and ^{3}H with kinetic energies of 573 and 191 keV, respectively (Fig. 1a). While slowing down and depositing their energies in the liquid, they will ionize ^{4}He atoms along their tracks [5].

Via recombination with an electron, an ionized atom forms a neutral excited molecule (excimer) He_2^* with a ground-state ^4He atom. While singlet excimers radiatively decay in 10 ns, triplet excimers are metastable with a long lifetime of $T_3 = 13$ s due to the forbidden spin-flip process. Thus, considering that the average energy of 42–43 eV for ionization does not depend much on the energetic particle and that the generation ratio of triplet excimers is roughly 50% [5], a localized cloud (cluster) consisting of 0.9×10^4 triplet He_2^* excimers with the size of 100 μm is expected to be generated by each n-^3He absorption reaction $^3He(n,p)^3H$.

For the proof-of-principle experiment in this proposal, the liquid helium sample (commercially available grade, without additional ^3He) was stored in a stainless steel dewar with four optical windows at the bottom part, where the diameter of helium bath is 160 mm and the size of each optical window is 30 mm in diameter (Fig. 1b). By depressurization, the temperature of liquid helium was kept at 1.8–1.9 K below the superfluid transition temperature, in order to avoid disturbance by vapor bubbles. The neutron beam for He_2^* excimer generation was introduced into liquid ^4He through a pair of the optical windows so as to minimize radioactivation of the dewar body.

To observe the generated He_2^* excimers, laser-induced fluorescence of triplet He_2^* excimer in liquid helium [6] was detected. By absorption of two 905 nm photons, a triplet excimer is excited from the lowest-energy state $a^3\Sigma_u^+$ to the excited state $d^3\Sigma_u^+$. The $d^3\Sigma_u^+$ state decays to the $b^3\Pi_g$ state, emitting a detectable 640 nm photon. When the $b^3\Pi_g$ state relaxes back to $a^3\Sigma_u^+$, the transition becomes cyclic and can be repeated during the lifetime $T_3 = 13$ s of the triplet He_2^* excimer. As the $b^3\Pi_g$ excimer often decays to vibrational levels of $a^3\Sigma_u^+$ off-resonant to 905 nm photons, "repumping" lasers exciting those insensitive excimers to $c^3\Pi_g^+$ state temporarily are additionally employed for faster relaxation. Since the excitation of 640 nm fluorescence is a two-photon process, an intensity of 0.4 MW/cm^2 at a pulse duration of 5 ns is required for saturation of the transition. To create such strong 905 nm laser pulses from 532 nm Nd:YAG pulsed laser, a fast wavelength converter using a Ti-sapphire crystal was newly developed in this project, of which details as well as the efficiency will be published elsewhere [7]. The 905 nm pulsed laser (0.7 mJ/pulse with a pulse duration of 4 ns) was overlapped with 1064 nm (300 mW) and 1085 nm (50 mW) CW lasers for repumping and aimed counterpropagating to the neutron beam. The resulting fluorescence of triplet He_2^* excimers was selectively observed by photomultiplier tubes (PMT) using 640 ± 5 nm bandpass filters, through two optical windows placed in the direction perpendicular to the neutron and laser beams. Acquisition of the PMT signals was triggered by the 905 nm excitation pulse photodiode signal and collected by a high-speed digital oscilloscope.

In the experiment using a continuous neutron beam at KUR, He_2^* excimer fluorescence was first confirmed, with a performance check of the developed optical system. And, a more quantitative experiment was conducted with improvements based on the knowledge obtained at KUR, using the pulsed neutron source of J-PARC/MLF. In the following sections, results of the latter experiment are shown.
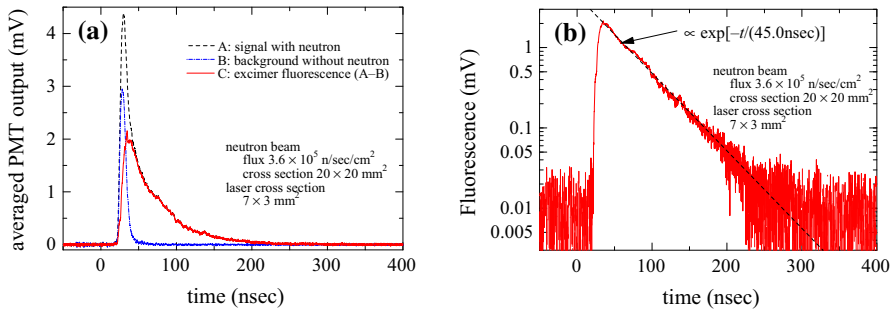
Fig. 2 Typical PMT signals where 2000 events triggered by the 905 nm excitation laser pulse are averaged, and a reproducible electrical noise is subtracted (see text). A delay of about 20 ns was caused by different signal path lengths. **a** Observed signals and extracted fluorescence signal. (Black) dashed line shows the signal when neutron beam is continuously applied. And (blue) dot-dashed line is the background in the case without neutrons. As a difference between them, fluorescence related to the neutron beam is extracted, which is plotted as (red) solid line. **b** Semilog plot of the fluorescence signal shown in (**a**). Fluorescence signal is plotted as (red) solid line. (Black) dashed line is a fitting of the decay. For all data, the function $a \exp(-bt)$ was directly fitted to the signal between 55 and 400 ns using an equally weighted nonlinear fitting. In the case shown, the derived time constant is $\tau (= 1/b) = 44.95 \pm 0.10$ (ns) (Color figure online)

3 Results on He$_2^*$ Excimers Generated by Neutrons

Figure 2a shows typical PMT signals when the neutron beam is either continuously applied or not applied, where 2000 events triggered by the 905 nm excitation laser pulse were averaged. In order to obtain the steady state for the number of He$_2^*$ excimers with the lifetime $T_3 = 13$ s, all data were taken at least 1 min ($\sim 5T_3$) after the main shutter for the neutron beam was open or closed. In raw signals corresponding to a single trigger event, a reproducible electrical noise (typically ± 0.7 mV) caused by the pump laser HV Q-switch was interfering with photon signals. The time profile of the noise was reconstructed by collection of no-photon regions from single events and averaging [7]. In signals shown in Fig. 2a, such electrical noise was already subtracted. As indicated by the (blue) dot-dashed line in the figure, a small amount of photons was always observed accompanying the excitation pulse in our experimental setup, even when neutrons were absent. Thus, subtracting those as a background from the observed signal shown by (black) dashed line, the fluorescence signal related to the neutron beam is extracted as (red) solid line. The semilog plot of this fluorescence signal is shown in Fig. 2b, to see the clear exponential decay. Since PMT spike signals of each photon were averaged in this signal, this curve indicates the probability of photon emission from the state excited by 905 nm laser, where the time constant τ is the lifetime of the excited state. Though the τ estimated by fittings shown in Fig. 2b scatters for various experimental conditions, the average and standard deviation are derived to be $\tau = 43 \pm 2$ ns. The τ is slightly shorter but comparable to 48 ± 2 ns previously reported for 640 nm fluorescence of triplet excimer He$_2^*$ [6]. Thus, this fluorescence indicates that τ is the $d^3\Sigma_u^+$-state lifetime of triplet excimers and that triplet excimers are generated when neutron beam is passing through liquid helium.

At the employed beamline BL22 of J-PARC/MLF, the neutron flux can be changed by the selection of upstream collimators and the main shutter apertures. The neutron
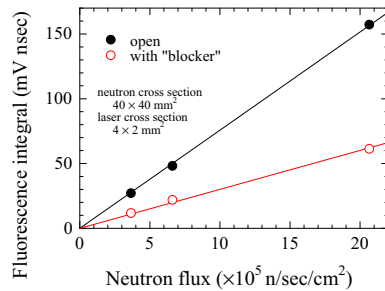
Fig. 3 Neutron flux dependence of fluorescence intensity from triplet He$_2^*$ excimers. Vertical axis is the time integral of fluorescence signals shown in Fig. 2. (Black) solid circles are those when the neutron flux is applied. Fluorescence proportional to the neutron flux indicates that all triplet He$_2^*$ excimers are generated directly or indirectly by applied neutrons. (Red) open circles are the case that "neutron blocker" was put on the neutron path. In this case, the horizontal axis is fluxes which should be applied if the blocker were not on the path. Actual neutron fluxes at the sample are significantly reduced by the blocker. Lines are linear fittings (Color figure online)

flux dependence of He$_2^*$ fluorescence intensity is plotted by (black) solid circles in Fig. 3. The fluorescence intensity is proportional to the neutron flux, which clearly indicates that all observed He$_2^*$ excimers are generated by the applied neutron beam.

4 Number of He$_2^*$ Excimers and Fraction Generated by Neutron-^{3}He Reaction

From the fluorescence signal intensity, the number of He$_2^*$ excimers can be roughly estimated. For the case that neutron flux is 3.6×10^5 n/s/cm^2 and laser cross section 4×2 mm^2, the number of detected He$_2^*$ fluorescence photons was 0.5–1.1 photons/event comparing to the dark current signal intensity. Though the number fluctuated probably due to influence of the background photons shown in Fig. 2a, the number was found to be independent of the starting time of liquid depressurization and the average was 0.9 photons/event. Referring to the low quantum efficiency of 0.5% for 640 nm and solid angle for the ϕ15 mm cathode of the employed PMT (Hamamatsu R750), the total number of fluorescence photons emitted in one event is estimated to be 5×10^5 ignoring losses at windows. As a single excimer is assumed to emit one photon in one event, the same amount of He$_2^*$ excimers should exist in the laser-sensitive volume $4 \times 2 \times 30$ mm^3, i.e., the density is estimated to be 2.0×10^6 excimers/cm^3.

On the other hand, the possible number of He$_2^*$ excimers can be also estimated from the n-^{3}He reaction rate. Since a pulsed neutron beam was applied, the energy range (0.002–0.4 eV) and distribution have been well determined by the time-of-flight measurement. Using the actual energy profile with the absorption cross section relation $\sigma = 5328(b) \times [\epsilon/0.0253(eV)]^{-1/2}$ for ^{3}He [8], the effective cross section for applied neutron beam is calculated to be $\sigma_{\text{eff}} = 9168(b)$. Assuming 0.3 ppm of ^{3}He in liquid He, which is typical in Japan, the reaction rate, i.e., generation rate of an He$_2^*$ excimer cluster, is estimated to be $f = 22$ clusters/cm^3/s for the flux 3.6×10^5 n/s/cm^2. Since the He$_2^*$ clusters are generated continuously during application of the neutron beam, at

the steady state where the generation and decay with the time constant of $T_3 = 13$ s are balanced, the average number of He_2^* clusters is $f T_3$, and the number of He_2^* excimers are estimated to be 2.6×10^6 excimers/cm^3 for expected 0.9×10^4 excimers/cluster.

Though agreement in the order of magnitude between both estimations seems to show their validity, the observed He_2^* excimers cannot be simply considered to be generated by the $^3He(n,p)^3H$ reaction. First, due to a difference in vapor pressures, ^3He vaporizes faster than ^4He in the depressurizing process of liquid He, especially until the temperature arrives at the superfluid transition temperature. It can cause significant reduction in the ^3He density. In addition, there is another neutron-related path to generate He_2^* excimers, which is indirect generation via γ-ray. Many materials can absorb neutrons and emit prompt γ-ray, and the γ-ray is known to generate He_2^* excimers via processes such as the Compton effect [5,9]. Though the reaction cross section is four orders smaller [10] and the resulting number of He_2^* excimers per reaction is one order smaller [5] than those of $^3He(n,p)^3H$, their contribution cannot be ignored since all He atoms may interact, not only ^3He.

Therefore, the γ-ray-generated fraction of He_2^* excimers was determined by control experiments. First, the effect of prompt γ-ray from materials around the cryostat was examined by variable cross section of the neutron beam. When the cross section is 20×20 mm^2, the full beam can pass through $\phi 30$ mm silica windows. In contrast, for 40×40 mm^2, 40% is absorbed by the shielding materials including boron carbide (B4C) around the cryostat, and 16% irradiates other materials around the windows. In each case, the fluorescence integral between 55 and 400 ns was obtained to be 16.0(9) and 15.5 mV ns, respectively. Thus, the contribution of these γ-rays was confirmed to be negligible within experimental errors. Next, to determine the effect of γ-rays coming from upstream together with neutron beam, we examined the case using "neutron blocker" which can be moved into the neutron path just before the experimental area. While the blocker made of polyethylene and B4C absorbs almost all of the neutron beam, it is transparent for γ-rays, and the intensity becomes even larger by prompt γ-ray from the neutron absorbent ^{10}B. The change in He_2^* fluorescence intensity by the blocker is shown by (red) open circles in Fig. 3, where the horizontal axis is the flux before the blocker was settled on the neutron path. The He_2^* excimer fluorescence significantly remains even when neutrons are blocked, but is reduced to be about 40%. This gives the upper limit of the γ-ray contribution to generate He_2^* excimers.

Thus, at least 60% of the observed He_2^* excimers, i.e., 1.2×10^6 excimers/cm^3, were confirmed to be generated by the n-^3He reaction $^3He(n,p)^3H$ for the neutron flux 3.6×10^5 n/s/cm^2. This corresponds to excimer clusters of 1.3×10^2 clusters/cm^3 if one cluster is simply considered to consist of 0.9×10^4 He_2^* excimers. The number of clusters increases with the neutron flux. It confirms that a sufficient number of He_2^* excimer clusters is available as tracers for visualization of the flow field in liquid He.

Although the number of He_2^* excimers for each cluster has not been determined yet, some speculations can be made. If the difference between the estimated number of observed He_2^* excimers and larger number estimated by the reaction rate is simply attributed to the reduction in ^3He density during depressurization of liquid He, the number of He_2^* excimers in one cluster is order of 10^4 as expected. However, ^3He density can be even lower depending on the experimental setup [11,12]. In such case,

the number will be larger. The actual number as well as the size of He_2^* clusters is an interest in future experiments.

And additionally, our result suggests a possibility of the ^{4}He-analog of experiments confirming the Kibble–Zurek mechanism in superfluid ^{3}He [13,14], with information of excimer generation. The relevant study is also of further interest.

5 Summary

We have confirmed generation of He_2^* excimers via the neutron absorption reaction of ^{3}He impurities in liquid ^{4}He, and the ability of detection by the laser-induced fluorescence. The generated number is estimated to be 10^6 excimers/cm^3 for the neutron flux 3.6×10^5 n/s/cm^2. From the order estimation, the number of He_2^* excimers in a cluster is expected to be about 10^4, so that the generated He_2^* excimers correspond to 10^2 clusters/cm^3. It was also demonstrated that the number of He_2^* clusters can increase proportionally with the neutron flux. Thus, the number of possible excimer clusters was confirmed to be sufficient as tracers for flow visualization in liquid ^{4}He. To determine the actual number of He_2^* excimers for each cluster and the cluster shape, visualization of the excimer cluster image by camera is desired as a next step.

References

1. W. Guo, M. La Mantia, D.P. Lathrop, S.W. Van Sciver, Proc. Natl. Acad. Sci. **111**, 4653 (2014)
2. W. Kubo, Y. Tsuji, J. Low Temp. Phys. **187**, 611 (2017)
3. A. Marakov, J. Gao, W. Guo, S.W. Van Sciver, G.G. Ihas, D.N. McKinsey, W.F. Vinen, Phys. Rev. B **91**, 094503 (2015)
4. D.E. Zmeev, F. Pakpour, P.M. Walmsley, A.I. Golov, W. Guo, D.N. McKinsey, G.G. Ihas, P.V.E. McClintock, S.N. Fisher, W.F. Vinen, Phys. Rev. Lett. **110**, 175303 (2013)
5. W. Guo, D.N. McKinsey, Phys. Rev. D **87**, 115001 (2013)
6. W.G. Rellergert, S.B. Cahn, A. Garvan, J.C. Hanson, W.H. Lippincott, J.A. Nikkel, D.N. McKinsey, Phys. Rev. Lett. **100**, 025301 (2008)
7. V. Sonnenschein et al., J. App. Phys. **(in preparation)**
8. K. Shibata et al., J. Nucl. Sci. Technol. **48**(1), 1–30 (2011)
9. J.D. Wright, W.G. Rellergert, S.B. Cahn, A. Curioni, J.A. Nikkel, D.N. McKinsey, J. Low Temp. Phys. **158**, 331 (2009)
10. M.J. Berger et al., XCOM: Photon Cross Sections Database, ver. 3.1, NIST Physical Measurement Laboratory. https://doi.org/10.18434/T48G6X
11. P.C. Tully, US Bureau of Mines Report of Investigation No. 8054 (1975)
12. B.V. Rollin, J. Hatton, Phys. Rev. **74**, 508 (1948)
13. C. Bäuerle, Yu.M. Bunkov, S.N. Fisher, H. Godfrin, G.R. Pickett, Nature **382**, 332 (1996)
14. V.M.H. Ruutu, V.B. Eltsov, A.J. Gill, T.W.B. Kibble, M. Krusius, Yu.G. Makhlin, B. Plaçais, G.E. Volovik, W. Xu, Nature **382**, 334 (1996)

Affiliations

T. Matsushita[1] ⓘ · **V. Sonnenschein**[2] ⓘ · **W. Guo**[3,4] · **H. Hayashida**[5] · **K. Hiroi**[6] ·
K. Hirota[1] · **T. Iguchi**[2] · **D. Ito**[7] · **M. Kitaguchi**[1] · **Y. Kiyanagi**[2] · **S. Kokuryu**[2] ·
W. Kubo[2] · **Y. Saito**[7] · **H. M. Shimizu**[1] · **T. Shinohara**[6] · **S. Suzuki**[2] ·
H. Tomita[2] · **Y. Tsuji**[2] · **N. Wada**[1]

[1]   Department of Physics, Nagoya University, Chikusa-ku, Nagoya 464-8602, Japan

[2]   Department of Energy Engineering, Nagoya University, Chikusa-ku, Nagoya 464-8603, Japan

[3]   Mechanical Engineering Department, Florida State University, Tallahassee, FL 32310, USA

[4]   National High Magnetic Field Laboratory, 1800 East Paul Dirac Drive, Tallahassee, FL 32310, USA

[5]   Neutron Science and Technology Center, Comprehensive Research Organization for Science and Society (CROSS), 162-1 Shirakata, Tokai, Ibaraki 319-1106, Japan

[6]   J-PARC Center, Japan Atomic Energy Agency (JAEA), 2-4 Shirakata, Tokai, Ibaraki 319-1195, Japan

[7]   Institute for Integrated Radiation and Nuclear Science, Kyoto University, 2 Asashiro-Nishi, Kumatori, Osaka 590-0494, Japan